Effect of *meta*-Carborane on Segmental Dynamics in a Bimodal Poly(dimethylsiloxane) Network

James P. Lewicki,[†] Robert S. Maxwell,*,[‡] Mogon Patel,*,[§] Julie L. Herberg,[‡] Anthony C. Swain,[§] John J. Liggat,[†] and Richard A. Pethrick[†]

Lawrence Livermore National Laboratory, Livermore, California, Department of Pure and Applied Chemistry, Westchem, University of Strathclyde, Glasgow, Scotland, and Atomic Weapons Establishment, Aldermasten, United Kingdom

Received July 11, 2008; Revised Manuscript Received October 14, 2008

ABSTRACT: Bimodal networks of polydimethylsiloxane (PDMS) filled with varying amounts of icosahedral *meta*-carborane (m-CB) have been developed and characterized by broadband dielectric spectroscopy (BDS) and static ^{1}H multiple quantum nuclear magnetic resonance (MQ NMR). Both BDS and MQ NMR showed evidence for a decrease in the polymer chain dynamics. BDS spectra quantified a normal-mode relaxation near 40 Hz at 40 °C. The frequency maximum observed for filled samples decreased with increasing m-CB content until contents greater than 5 wt %. The width of the relaxation spectrum increased with the addition of small quantities of filler and decreased with filler contents greater that 5 wt %. Agglomeration effects were observed at loadings greater than 5 wt % as manifest by the onset of low frequency Maxwell–Wagner–Sillars (MWS) processes. The MQ NMR data allowed the characterization of distributions of the residual dipolar couplings, $<\Omega_d>$ and, thus, in the dynamic order parameter, S_b, consistent with the bimodal network architecture expected from the synthesis protocol used. Upon addition of less than 10 wt % m-CB filler, the mean $<\Omega_d>$ for the longer chains increased by 46% and the width of the distribution increased by 33%. The mean $<\Omega_d>$ for the shorter chains increased by much less, indicative of preferential dispersion of the filler particles in the long chain domains of the network structure. We conclude that the mechanism of reinforcement is likely free volume space filling at low loadings transitioning to complex molecular filler and polymer chain interaction phenomena at higher loadings.

Introduction

Polymer–nanoparticle composites have been gaining increasing interest in the last few decades due to significant potential advantages over traditional polymer–filler composites, including enhanced mechanical and chemical properties.[1,2] Significant improvements in mechanical reinforcement over what is predicted from simple mixing theories have been realized using nanoscale fillers instead of traditional macroscale fillers such as silicas and carbon black. The addition of nanoparticles with novel chemical, optical, or barrier properties further opens the door to the development of so-called multifunctional materials. Despite broad interest, however, there is still uncertainty in the mechanism of reinforcement preventing rational control and optimization of properties for numerous engineering and chemical applications. It has been hypothesized, for example, that, like traditional macroscale fillers, the reinforcement may be due to the formation of physical topological constraints via surface interactions (e.g., hydrogen bonds or van der Waals interactions).[3] In nanocomposites, such surface interactions are significantly increased in efficiency due to more compatible size between the polymer and the filler and the dramatic increases in available surface area for given volume fraction.[4] Ozmusul et al., however, suggested that the observed improvements in mechanical properties were due to the formation of a long-lived, yet transient, filler network mediated by the polymer chains (e.g., filler particles sufficiently close so polymer "bridges" between particles can form), thus, increasing the efficiency of the polymer network in relieving local strain.[5]

The segmental dynamics and local order underlie much of the fundamental physics that influence the performance of

elastomers and can serve as important diagnostics for reinforcement and other fundamental properties (e.g., network topology, cross-link density, the number and distance between chemical and physical (entanglements) cross-links, the type and volume fraction of filler).[6,7] Thus, characterizing the dynamics and order can provide key insight into structure–property relationships and the mechanisms of reinforcement. Some early experimental and computational work on nanocomposites has suggested that presence of filler particles would be expected to perturb chain conformation.[8–10] Recent simulations and experimental work, however, while observing perturbations to the small fraction of bridging chains, have suggested that this is not the case and predicted little to no effect on the conformation or end-to-end vector length of bulk polymer chains due to the addition of spherical nanofillers with or without strong polymer–filler interaction, apparently on any scale.[5,11–15]

A number of techniques have been developed to directly probe the segmental dynamics in polymeric materials, including broadband dielectric spectroscopy (BDS). BDS is a form of relaxation spectroscopy that can be utilized to study varied relaxation phenomena in polymeric systems. BDS studies of polymer systems possessing permanent net dipole moments typically focus on the α-relaxation behavior of the polymer over the region of T_g.[16] Despite the fact the dipolar motion of the α-process is typically described as independent of segmental motion, the physical rotation of a main chain segment requires a significant level of co-operative motion from neighboring chain segments and an increase in free-volume of the system in order to occur and is therefore *not* an isolated process. The observation of the α-relaxation correlates with the onset of cooperative motion and the rate-change in free volume expansion that occurs at T_g means that an examination of this segmental process can yield information on the relative mobility and chain dynamics in a polymer system. The α-relaxation of PDMS has been studied in detail and the effects of fillers (both micron and

* To whom correspondence should be addressed. Tel.: (925) 423 4991(R.S.M.). E-mail: maxwell7@llnl.gov (R.S.M.); mogon.patel@awe.co.uk. (M.P.).
† University of Strathclyde.
‡ Lawrence Livermore National Laboratory.
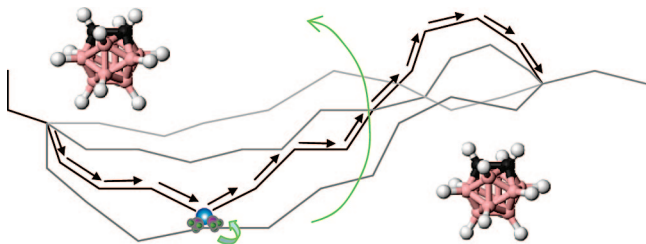§ Atomic Weapons Establishment.

Figure 1. Illustration of the coupling between the alpha and beta relaxation modes in polysiloxanes with *meta*-caborane (m-CB) nanoparticles. Icosahedral m-CB is nominally 5 nm in diameter. Black arrows symbolize chain dipole vectors. Green arrow symbolizes large scale chain dynamics that perturb both the chain dipole vectors (long arrow) and the preaveraged ^{1}H dipolar couplings of the protons in the >$Si(CH_3)_2$ groups (short arrow).

nanoscale) on the segmental dynamics of PDMS systems as a function of the α-relaxation have also been studied.[17,18]

BDS can also be employed to study interfacial, rather than dipolar polarization phenomena in polymeric systems: In heterogeneous polymer systems with a crystalline or filler phase present in the bulk, *interfacial polarization phenomena* can be observed under an applied electric field, resultant from the accumulation of virtual charges at the interface between the bulk and secondary phases. This class of polarization phenomena are often termed Maxwell−Wagner−Sillars (MWS) processes. MWS processes can be observed as distinct relaxations with frequency domain dielectric spectroscopy. The strength and relaxation time of the process is dependent on many factors including the mass fraction, morphology, and conductivity of the secondary phase; therefore, MWS relaxations can potentially yield valuable information on the nature of a dispersed or secondary phase within a polymeric system. The effective charge distance in MWS processes is of 10 orders of magnitude greater than for a typical molecular dipole therefore MWS relaxations are typically observed at significantly lower frequencies than dipolar relaxations.[42]

In this work, however, the *normal-mode* relaxation behavior of PDMS is of interest. Such higher order cooperative relaxation behavior can be observed in polymeric systems above their T_g when both the directional and electric vectors of the chain dipoles are identical; the resultant motion of the polymer is therefore a cooperative global movement described in terms of a normal-mode of motion (as illustrated in Figure 1). Experimentally, the normal-mode relaxation is often difficult to observe in polymer melts or elastomer systems above T_g due to the difficulties that arise in resolving the relaxation from the strong dipolar contributions at these temperatures. Despite the experimental difficulties encountered, the normal-mode relaxation is potentially interesting as it can yield information over a size scale greater than that of the α-segmental motions. By taking advantage of the low ionic conductivity of PDMS systems and the net dipole due to the overall asymmetry of the backbone, it is possible to observe a normal-mode relaxation of PDMS at temperatures well in excess of T_g.[43] This work demonstrated the observation of normal-mode motion in PDMS liquids and solutions using a combination of high frequency ultrasound and dynamic viscoelastic measurements, concluding that both the viscoelastic and low frequency ultrasonic relaxations observed derived from normal mode motions of the polymer chains. Furthermore, this work demonstrated that the normal mode relaxation times were dependent on the constraints placed upon the polymer chains. It is our assertion that the comparatively large magnitude and slow relaxation observed in the melt is indeed indicative of normal-mode motions of the PDMS main chain. This relaxation bears no strong resemblance to a MWS effect; occurring over the frequency range that it does and is

not associated with large ionic conductivity contributions. Cross-linking of the PDMS systems would not necessarily be expected to eliminate normal mode motion in a PDMS network such as this, where individual chains can be over 1000 units in length and the backbone will still have considerable freedom of motion, including reptation over length less than the average chain length of the low cross-link density chains. Significant motion of both monomers within chains as well as the cross-linking junctions themselves have been predicted and observed experimentally, particularly by neutron spin−echo spectroscopy.[44−47]

The potential advantage of examining the normal-mode relaxation process in PDMS nanocomposite systems is that the size scale of this relaxation is such that the motion of the chain segments will be highly coupled to changes in the free volume of the composite system. Therefore, an examination of normal-mode relaxation has the potential to yield information on the effects of low levels of nanoparticles on the chain dynamics, free volume and plasticization of a siloxane matrix. Indeed, recent work by the authors has demonstrated the utility of BDS normal-mode relaxation observations as a tool for probing subtle filler-induced changes in the chain dynamics of PDMS/POSS nanocomposite systems.[19]

Nuclear magnetic resonance (NMR) has also been extensively used to characterize segmental dynamics and order in polymeric systems primarily through quantification of residual dipolar couplings.[20−22] For elastomeric systems, the residual dipolar couplings typically are due to incomplete averaging of aniso-tropic magnetic interactions that serve to broaden static NMR spectra of solids. This incomplete averaging is, in turn, caused by topological constraints interfering with fast isotropic reori-entations on the NMR time scale. The residual dipolar couplings strongly depend on the mechanisms and timescales of the complex motional processes present in elastomer melts. Residual dipolar couplings, as a result, can be used to test theories of elasticity, gelation, and polymer conformation, as well as provide insight into the network structure.

A number of NMR methods are available to quantify the residual dipolar couplings.[23−33] The most popular spin−echo based methods often overestimate the residual dipolar couplings and, thus, the dynamic order parameters. Recently, it has been reported that the characterization of the growth of multiple quantum coherences can provide detailed insight into silicone network structure by increasing the selectivity of the NMR experiment to the structure and dynamics most connected to the topology of the polymer network, including chain ordering in the bulk and at the surface of inorganic filler par-ticles.[22,24,26,27,30,31,34−38] These methods have been used recently to probe structural order in a series of monomodal and bimodal model networks, as well as a number of traditional filled complex silicone networks.[30,31,34−38] Because the network topology and the filler−particle interactions determine to a significant part the engineering properties including tensile, shear, and creep moduli, multiple quantum (MQ) methods offer the potential for model free insight into the origins of material performance.[3,6,7] The normalized MQ NMR procedure used here has been shown to effectively remove contributions due to rapid and slow motional processes that complicate spin−echo based studies and provide results due to the ms time scale motions most associated with normal mode segmental dynamics.[22] Given the ability of the MQ NMR methods to quantify changes to segmental dynamics in more traditional filled polymer systems (due to factors such as changes in network structure, filler content, interfacial bonding, and strain) the method should be able to provide additional insight into the mechanisms of reinforcement in silicone based nanocomposites. To date, however, it has not been used to characterize segmental dynamics in such systems, particularly systems with spherical

nanoparticles where much of the computational effort has been focused.

Here we employ both BDS and MQ NMR to characterize the changes in polymer structure and dynamics in a bimodal PDMS resin filled with spherical boron cluster nanoparticles called icosahedral *meta*-carboranes (m-CB, see Figure 1). These boron containing compounds, generally expressed by the molecular formula $C_2B_nH_{n+2}$, exhibit rather specific properties, in particular, high thermal stability and chemical stability, and show unusual chemistry not encountered in other materials.[39] Most importantly, these relatively novel particles can be exploited for developing advanced multifunctional materials with tailored mechanical, physics and engineering properties via alteration of the interfacial interactions strength through modification of the organic functionality of the nanoparticle or incorporation in either blends or cross-linking modalities. Potential applications of such materials may be found in sensing, energy release, and aerospace/military applications.

Experimental Section

Sample Preparation. Poly(dimethylsiloxane) (PDMS) resin materials were made into foamed pads or solid elastomers about 2 inches in diameter using standard silicone cure chemistry using a bimodal distribution of two average PDMS chain lengths.[40] Cross-linking was accomplished with stoichiometric quantities of tetrapropoxysilane (TPOS) in the presence of 5% tin(II) 2-ethyl(hexanoate) catalyst. Typical formulations were 10.333 g high molecular weight (HMW) PDMS ($M_n \sim 77000$ g mol^{-1}), 4.6663 g low molecular weight (LMW; $M_n \sim 550$ g mol^{-1}) PDMS, 1.1375 g TPOS, and 0.75 g Sn catalyst. The methodology of sample prep was typically as follows: 10.333 g of HMW PDMS was mixed with 4.666 g of LMW PDMS by an IKA-Werke overhead stirrer, at which point the appropriate mass of m-CB suspended in THF was added and mixed mechanically (using a Speedymix blender) for 20 min. The resin blend was then degassed and cooled to 2 °C. A stoichiometric quantity of TPOS was mechanically mixed into the blend. Finally, 5% of tin(II) 2-ethylhexanoate catalyst was mixed into the blend and the mixture was transferred into a 10 cm^2 mold. This was cured in an oven at 65 °C for 20 min. The elastomer that was formed was removed from the mold and postcured for a further fifteen hours at 65 °C. m-CB was purchased from the supplier (Katchem Limited), all other chemical components were purchased from Sigma-Aldrich U.K. The mean particle diameter of the carborane cage is typically 5 nm, and good dispersion (at low loading, <5%) is expected due to our use of a common solvent to dissolve the particles before adding and mixing the solution into the siloxane.

Stress−strain curves and mechanical property data were obtained in air at 35 °C using a TA instruments Q800 Dynamic Mechanical Analyzer (DMA) operating in static mode (no frequency). DSC thermographs were obtained in air typically at 10 °C/min heating rate using a TA Instruments 2940 differential scanning calorimeter. Glass transition temperatures were observed at −123 ± 5 °C. No difference within experimental error in T_g with increasing carborane content was observed.

BDS. The instrument used for the BDS analysis of all solid elastomer systems was a Strathdow Dielectric Spectrometer. This instrument was based upon a Solartron SI 1250 Broadband Frequency Response Analyzer. The instrument had a working frequency range of 10^{-3} to 6.5×10^5 Hz. All BDS analyses reported in this paper were carried out using a computer controlled frequency domain method (as described by D. Hayward et al.[41]). All solid elastomer samples were analyzed in a parallel plate cell with a working circular sample diameter of 25 mm. Sample temperature control of ±0.1 °C was obtained by means of an internal silver block containing a platinum resistor, heating element and liquid N$_2$ channel all managed by an external computer controller and pump. Liquid samples were analyzed using a Solartron SI 1260 Impendence/Gain-Phase Analyzer and Novacontrol Broadband Dielectric Converter. This instrument had a frequency range of 10^{-3}
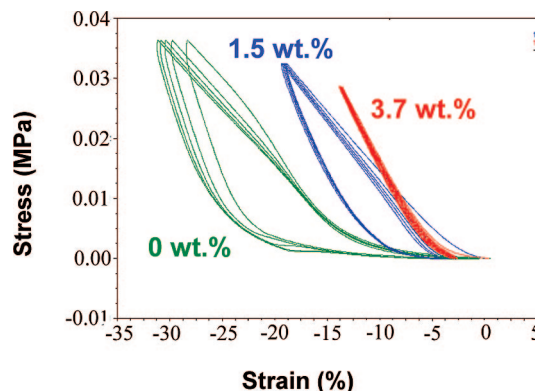

Figure 2. Results from thermomechanical analysis studies showing the dramatic influence of m-CB particles on polymer hysteresis (red, 3.7 wt % loading; blue, 1.5% wt loading and green is the nonfilled material).

to 10^6 Hz. Liquid cells were analyzed in a liquid capable parallel plate cell with an effective circular sample diameter and thickness provided by the electrodes of 25 and 1.5 mm, respectively. Sample temperature control of ±0.1 °C was obtained by means of a Novatherm active controlling heated sample chamber.

PDMS has a net dipole moment as a result of the polar Si−O bond and the asymmetry of the chain backbone. It is possible to resolve an α-segmental relaxation for PDMS (typically observed at ∼500 Hz at −125 °C), however it is necessary to quench the polymer to temperatures below T_m so as to prevent crystallization of the sample and inhibition of the α-process. The normal mode relaxation of the PDMS chains was of interest in this study and it is generally observed at temperatures well above the T_g of PDMS (−123 °C). Therefore, all BDS analyses of the samples were carried out at temperature of 40 °C. The normal mode has been observed in soluble PDMS chains and in uncrosslinked melts previously due to the permanent dipoles of the polar Si−O bond and the overall backbone asymmetry. In a random coil configuration, individual dipoles are capable of forming a net dipole over several units. In PDMS networks far above T_g, there is significant motion of both the polymer chains between cross-links (∼1000 monomers between cross-links in the low cross-link density domain) and the cross-links themselves, as has been observed by neutron spin−echo experiments.[44] At these temperatures, however, there are significant dipolar conductivity contributions to the loss components of the dielectric spectra. There is also a large scale MWS interfacial polarization response in the samples at these temperatures, which is attributed the stannous oxide particles (a catalyst residue) present within the matrices and other ionic residues.[42] As a result of this, the normal mode relaxation due to the stannous oxide has to be decoupled from the overall response. This was achieved experimentally by separating the complex experimental data into components of ϵ', ϵ'', and σ using an empirical minimization function running from MathCAD. The software was therefore able to resolve the normal mode relaxation as a fitted Havriliak−Negami (H−N) curve.[48] The program used a Levenberg−Marquardt routine to arrive at parameters which fit one or more H−N dispersion curves to the experimental data (it has been found that minimizing on the modulus of the complex permittivity gives the most stable solutions). This form of minimization function is similar to that developed by J. R. Macdonald who has developed several similar minimization routines for obtaining solutions to complex dielectric spectra.[49]

NMR. All MQ NMR experiments were performed on a Bruker Avance 400 spectrometer with a ^{1}H frequency of 400.013 MHz. Small samples (∼10 mm^3) were centered within the coil volume of a Bruker TBI (HCX) 5 mm probe with 90° pulse lengths $\tau_p =$ 4.50 μs. The refocused pulse sequence of Baum and Pines was used to generate and detect multiple quantum coherences.[30,50] The detected coherences, containing all excited $2n+2$ quantum orders, were selected using a four-step reconversion phase cycle with 90°

Table 1

sample	G' (MPa)	hyst width	f_{max} (Hz)	$<\Omega_d>_{low}$ (krad/s)	σ_{low} (krad/s)	$<\Omega_d>_{high}$ (krad/s)	σ_{high} (krad/s)
unfilled	0.19	5.5	0.44	0.7	0.15	4.0	1.0
1.5 wt %	0.23	2.25	0.15	1.27	0.20	4.5	1.0
3.7 wt %	0.32	0.33	0.15	1.3	0.20	4.5	1.0
35 wt %	0.34	1.25	0.05	1.0	0.15	4.0	1.0

steps while phase inverting the receiver on alternate scans. In addition, the read pulse and receiver were synchronously incremented in a CYCLOPS fashion to yield a sixteen-step phase cycle. Reference MQ coherences, containing all excited 4n quantum orders, were selected using the DQ selection phase cycle without receiver alternation. All experiments were performed by incrementing the DQ mixing time, $\tau_{DQ} = a(\Psi)n_c t_c$, via incrementing the loop counter n_c with cycle times, t_c, of ~180 μs. The finite nature of the radio frequency pulses were compensated for using the scaling factor $a(\Psi) = 1-12\ \tau_p/t_c$ rigorously derived elsewhere.[30] The MQ growth curves were normalized dividing the intensity of the MQ signal, I_{mq}, by the sum $I_{ref} + I_{mq}$, where I_{ref} is the intensity of the pulse sequence with the phases of the detection pulses modified to collect the entire transverse magnetization.

It has been shown that the growth of the normalized signal, S_{dq} can be related to the sum of terms for each site of a distribution of residual dipolar couplings, $<\Omega_d>$, where[30]

$$S_{dq} = \sum P_I \cdot I_{nDQ}(<\Omega_d>_I, \tau_{dq}) \quad (1)$$

where P_i is the population of spins described by residual dipolar coupling $<\Omega_d>_i$ and the contribution to the growth curve for each $<\Omega_d>$ within the second-moment approximation is given as an inverted Gaussian with the following form

$$I_{nDQ}(<\Omega_d>;\tau_{DQ}) = 0.5 \times (1 - e^{-\frac{2}{5}<\Omega_d>^2\tau_{DQ}^2}) \quad (2)$$

Here it is assumed that $<\Omega_d>$ follows static Gaussian statistics. Saalwächter et al.,[30] Gjersing et al.,[34] and Giuliani et al.[35] have shown that for a number of common silicone networks the distribution of $<\Omega_d>$ can be approximated as Gaussian

$$I_{nDQ}(<\Omega_d>,\sigma_d;\tau_{DQ}) = 0.5 \times \left(1 - \frac{e^{-\frac{\frac{2}{5}<\Omega_d>^2\tau_{DQ}^2}{1+2\frac{2}{5}\sigma_d^2\tau_{DQ}^2}}}{\sqrt{1+2\frac{2}{5}\sigma_d^2\tau_{DQ}^2}} \right) \quad (3)$$

where $<\Omega_d>$ and σ_d are the average dipolar coupling and distribution width, respectively.

Further, it has been shown that the residual dipolar couplings can be related to the dynamic order parameter and thus the average end-to-end vector and the number of statistical segments between effective cross-links (either chemical or physical), as illustrated in Figure 1.[20,21]

$$S_b = \frac{1}{P_2(\cos\alpha)}\frac{\langle\Omega_d\rangle}{\langle\Omega_d\rangle_{static}} = \frac{3r^2}{5N} \quad (4)$$

where $<\Omega_d>_{static}$ is the dipolar coupling in the absence of motion (but preaveraged by the fast motion of the methyl group) and equal to 8900 Hz, $<P_2(\cos\alpha)>$ is the time-averaged second order Legendre polynomial of the angle between the dipolar vector and the chain axis (i.e., the angle between the backbone chain axis and the Si–C vector), and r is the vector describing the deviation of the end-to-end vector, **R**, from that of the unperturbed melt, **R**$_o$: $<r^2 = <R^2>/<R_o^2>$.[34]

Results

Thermomechanical Studies. Stress–strain curves obtained from compression for unfilled and filled samples are shown in Figure 2 and show a loading level dependence on the equilib-
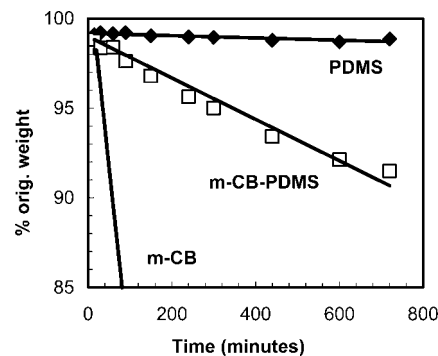

Figure 3. Weight loss studies at 75 °C for (◆) unfilled sylgard, (□) m-CB filled bimodal PDMS network (30 wt % loading), and (-) pure m-CB. The m-CB particles are relatively mobile within a siloxane matrix.

rium compression modulus, G'. The equilibrium compression modulus was observed to increase approximately 67% with only 1.5 wt % m-CB added, but the degree of change in modulus for a given increases in filler content was significantly reduced for higher filler content (see Table 1).

The stress strain curves also reveal a significant amount of hysteresis (hyst) for all samples, and is dependent on the filler loading level, as shown in Figure 2 and Table 1. Such hysteresis is typically observed in filled and unfilled silicone polymers and is the result of viscoelastic chain slippage and rearrangement effects within the network. The width of the stress–strain curve at 50% maximum stress also shows a dramatic decrease in the degree of hysteresis. The m-CB particles presumably are binding PDMS chains through weak interfacial interactions causing a reduction in the rate of processes that influence hysteresis.

Results of isothermal thermogravimetric analysis (TGA) measurements at 75 °C on bulk PDMS (in this case a commercial silicone, Sylgard 184), bulk m-CB, and m-CB mixed into the bimodal PDMS network studied here is shown in Figure 3. The TGA data shows that m-CB particles are significantly mobile within the PDMS matrix, though not as volatile as pure m-CB. The presence of the siloxane matrix, likely through interfacial interactions with the m-CB, hinders the mobility and loss of the filler. The small weight loss seen in the pure siloxane matrix arises from loss of cyclic volatiles, through well-known degradation mechanisms.[51–54]

BDS Results. The (unrestricted) normal-mode motion of PDMS has been initially characterized in the liquid state. Figure 4 shows the resolved normal-mode relaxation spectrum of the high molecular weight hydroxy-terminated PDMS polymer (M_n = 77000 g mol^{-1}) at a series of temperatures from 25 to 50 °C. As expected, the relaxation exhibits a strong temperature dependence; showing an approximate three decade shift in f_{max} over a 25 °C range. The apparent activation energy for this process was determined by plotting log[f_{max}] versus $1/T$ (K), and was found to be linearly dependent. The linear dependence demonstrates that the normal mode relaxation kinetics is pseudo-Arrhenius, a direct consequence of the freedom of motion of the PDMS chain which has a minimal degree of interchain interactions. The apparent activation energy for the observed relaxation in the PDMS liquid was determined to be ~42 ± 1 kJ mol^{-1}. This value is comparable (30–35 kJ/mol) to that measured by Patel et al. from TMA based stress relaxation studies on similar standard silica filled PDMS samples and is typically characteristic of physical relaxation processes within the polymer.[54]

The effect of cure on the normal-mode relaxation was investigated and the relaxation spectra of the uncured polymer and the cross-linked PDMS matrix are compared in Figure 5
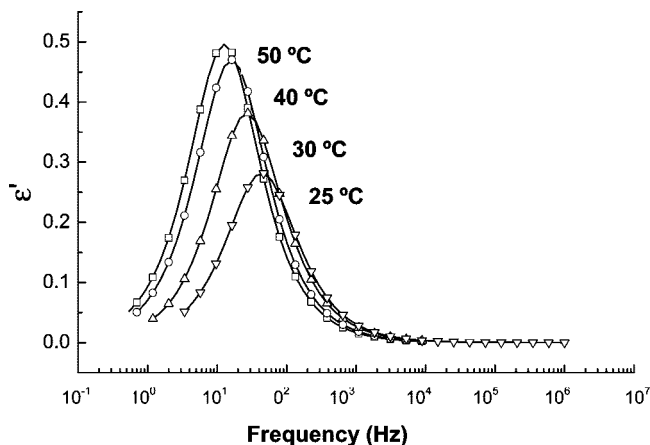
Figure 4. Resolved normal-mode relaxation of a hydroxy-terminated PDMS liquid (M_n = 77000 g mol^{-1}) exhibiting typical temperature dependent relaxation behavior. Squares, circles, up-triangles, and down-triangles correspond to temperatures of 25, 30, 40, and 50 °C, respectively.
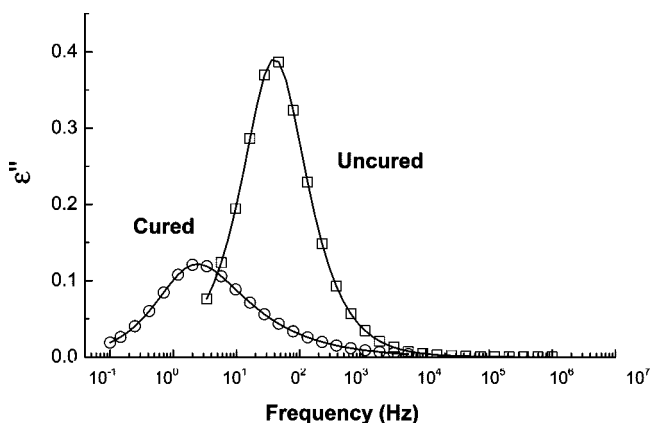

Figure 5. Comparative relaxation behavior of uncured and cured PDMS at 40 °C. Squares and circles represent the uncured and cured systems, respectively.

and show that polysiloxane cure significantly influences the normal mode relaxation properties. It can be observed that at a temperature of 40 °C the uncured, liquid PDMS resin exhibits a distinct relaxation at f_{max} = 36 Hz. Cross-linking of this system results in more than an order of magnitude shift in f_{max} to lower frequencies and an asymmetrical broadening of the relaxation which is indicative of a significant reduction in chain mobility.

Our BDS studies also show that the introduction of m-CB into the PDMS network affects chain mobility, influencing the normal mode relaxation process. The relaxation behavior of the unfilled PDMS matrix and the three m-CB filled elastomers are compared in Figure 6A and the trends in f_{max} are shown in Figure 6B. The BDS data show a clear trend of decreasing chain mobility with increasing filler loading. Furthermore, at the highest loading (>5 wt %) of m-CB a low frequency interfacial polarization Maxwell−Wagner−Sillars (MWS) relaxation process is present as obtained from the nonresolved permittivity/loss spectra shown in Figure 7.[42,55] The low frequency MWS loss is typical of agglomerated or poorly dispersed filler particles. Because m-CBs show relative high mobility within a siloxane matrix, for consideration for long-term technological applications, they would need to be bound covalently to otherwise prevent agglomeration and migration. This is particularly true in cases of high loadings as the nanoparticle−nanoparticle distances become, on average, short enough that the interaction potential for agglomeration overcomes the drivers for dispersion.[56,57] At these high loadings, full nanoscale dispersion and
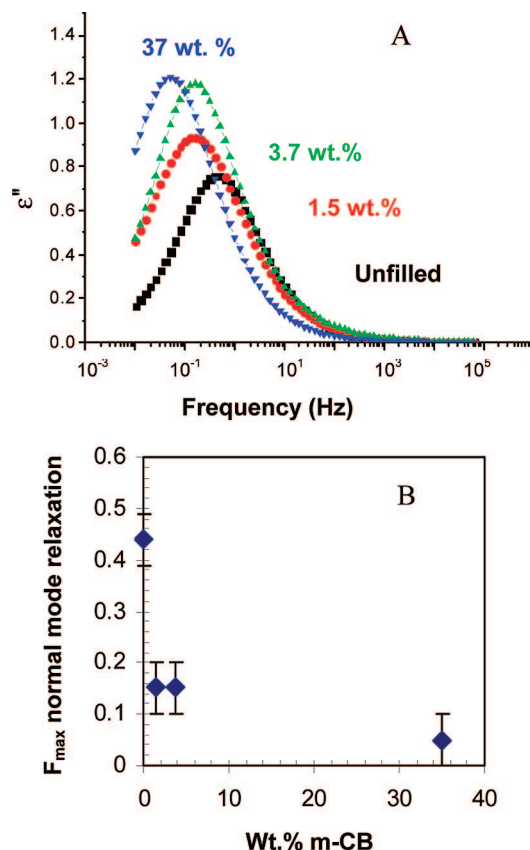

Figure 6. (A) Resolved relaxations of unfilled and m-CB functionalized PDMS elastomers derived from BDS measurements at 40 °C. f_{max} for the relaxation is observed to shift to lower frequencies with increasing m-CB loadings. Squares, circles, up-triangles, and down-triangles correspond to the unfilled, 1.5 wt %, 3.7 wt %, and 35 wt % m-CB filled systems, respectively. (B) Trend in f_{max} with increasing m-CB loading for the m-CB functionalized PDMS elastomer systems.
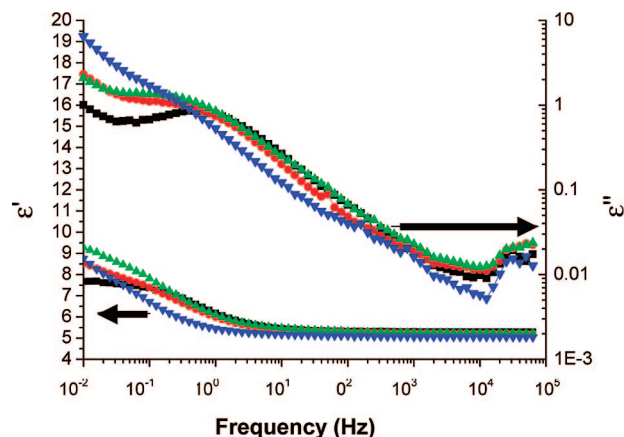

Figure 7. Complex BDS real and imaginary permittivity data for m-CB functionalized PDMS elastomer systems. Squares, circles, up-triangles and down-triangles correspond to the unfilled, 1.5 wt %, 3.7 wt %, and 35 wt % m-CB filled systems, respectively. A low frequency MWS process is observed as a component of the 35 wt % m-CB data.

incorporation into the network is not achieved and larger agglomerated particles are formed which are capable of inducing measurable interfacial polarization effects. Indeed, such MWS polarization effects similar to these have been observed by the authors in nanoclay filled polysiloxane networks-where filler network formation leads to agglomeration of clay particles.[58]

NMR Results. Room temperature, static ^{1}H MQ NMR growth curves are shown in Figure 8 for pristine and m-CB
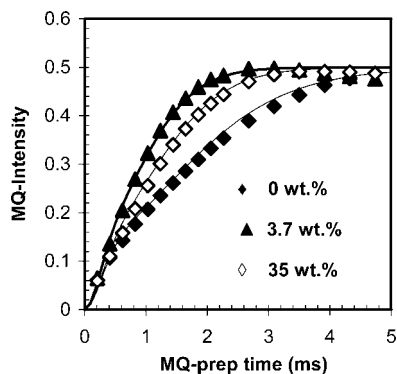
Figure 8. Normalized MQ NMR growth curves for m-CB-bimodal PDMS composites.

filled bimodal PDMS networks. The growth curves show distinct evidence for dual components: a higher $<\Omega_d>$ that dominates for $\tau_{mq} < 0.75$ ms and a lower residual dipolar coupling component that dominates for $\tau_{mq} > 0.75$ ms. In all cases, the filled materials were characterized by an increase growth rate both at early and long multiple quantum growth times, indicating a decrease in the amplitude of the segmental dynamics upon addition of the m-CB. None of the measured growth curves could be adequately fit to eqs 1 and 2 using a simple two site model. Fits to eqs 1 and 3 assuming two domains with Gaussian distributions of $<\Omega_d>$s were obtained and the histograms are shown in Figure 9A. Previous MQ NMR studies of silicone networks have shown similar Gaussian or near-Gaussian distributions of $<\Omega_d>$ and dynamic order parameters.[30,31,34,35] For all samples, a distribution near 1 krad/sec with a population contribution near 70% and a distribution centered at ~4 krad/sec with a population distribution of ~30% were obtained. The populations are consistent with that expected from the starting materials (67 mol% of monomers are from the high molecular weight chains). The low residual dipolar coupling domain is assigned to the long polymer chains with MW ~ 77000 g/mol. Eq 4 would predict $S_b \sim 0.0034$ rather than that found here of ~ 0.023 for the unfilled polymer. This discrepancy is due to

the additional topological constraints due to engagements ($MW_c \sim 11000$ g/mol: $S_b \sim 0.024$).[34] The high residual dipolar coupling domain is due to the short PDMS chains (MW ~ 750 g/mol: $S_{b-theory} = 0.34$ for a network of short chains only versus $S_{b-expt} = 0.15$). In this case, the predicted and observed dynamic order parameters are within reasonable agreement with the discrepancy likely due to increased mobility afforded by the longer chains. The mean and width of $<\Omega_d>$ as a function of filler loading are shown in Figure 9B. Upon addition of small amounts of m-CB filler (<10 wt %), the mean $<\Omega_d>_{low}$ and order parameters were observed to increase by ~46% while the width increased slightly less (~ 33%). $<\Omega_d>_{high}$ increased by a significantly less amount (~13%) and the width remained unchanged. The lack of observable change in the parameters associated with the lower molecular weight chains are likely the result of quantifying changes in the growth curve where it is represented by only three data points. A preferential increase, however, in $<\Omega_d>_{low}$ is not surprising given the expected reduced free volume in the low MW chain domains. For the network filled with 35 wt % filler, the mean $<\Omega_d>$ and S_b were observed to decrease from the high values found for the 5 wt % filled composite and narrowed in width to a level between the unfilled and the 1.5 wt % m-CB filled sample.

Discussion and Conclusion

As shown above, upon the addition of small quantities of m-CB to a bimodal silicone network, significant changes were observed in the compressive modulus, the degree of hysteresis observed in compression between loading and unloading, in the f_{max} and spectral width observed by BDS, and in the mean and width of the distributions in the residual dipolar couplings and dynamic order parameters obtained by MQ NMR.

The nanometric m-CB fillers are obviously effecting how the composite responds to load. The change in hysteresis implies a time dependence consistent with the formation of filler-polymer network interactions. The TGA results are consistent, as well, with significant filler-polymer interaction strength. BDS analysis of the m-CB/PDMS composite systems has shown that the introduction of increasing levels of m-CB into the siloxane
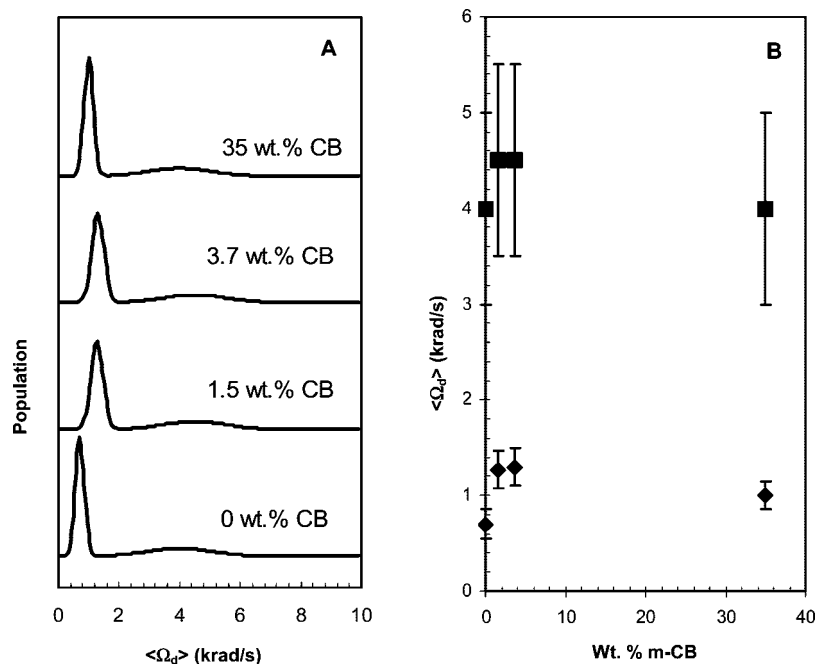

Figure 9. (A) Distributions of $<\Omega_d>$ obtained from fitting growth curves in Figure 8 to eqs 1 and 4 for m-CB blended into a bimodal-PDMS network; (B) $<\Omega_d>$ as a function of m-CB content in bimodal PDMS composites. Error bars in (B) represent width of the Gaussian distributions shown in Figure 9A.

network shifts the f_{max} value of the normal-mode relaxation significantly toward lower frequencies, indicative of a corresponding decrease in the freedom of motion of extended segments of the PDMS chains. Thus, incorporation of low levels of nanoscale m-CB particles alters the chain dynamics of a cross-linked bimodal PDMS network. MQ NMR also has shown a decrease in the amplitude of the segmental dynamics though an increase in both the mean $<\Omega_d>$ and the width of the distribution of $<\Omega_d>$, particularly for the longer chains in the bimodal network. In such self-reinforcing bimodal networks there is some evidence that a certain degree of phase separation occurs and that the short chain segment form highly cross-linked clusters.[22,59] Because it is expected that significantly more free volume is available in the longer chain domains, the preferential dispersion of the filler particles in this domain is not surprising. Such changes in f_{max} and $<\Omega_d>$ could be due to (1) change in effective $1/N$ (i.e., cross-link density) or (2) a change in orientational order due to presence of filler particles. Computational studies on spherical nanoparticle filled composites to date have shown no significant influence of filler on average segmental end-to-end distance, though perturbations at the filler surface have been identified.[8–10] Modeling of such networks also has shown no long-term changes to the order parameter would occur.[11–15] Formation of topological constraints may be occurring through weak long-range interactions, electrostatic or van der Waals, which would be expected to contribute to reducing the segmental dynamics and increasing dynamic order parameter while introducing mechanisms by which efficient stress can be relieved upon loading, for example, the decrease in load−unload hysteresis observed under compression. Such interactions would also be consistent with the decreased volatility of m-m-CBs in a silicone matrix.

We postulate that the primary mechanism of reinforcement at low fill level is one of "space filling", whereby the nanoscale m-CBs are on the correct size scale to effectively occupy free-volume within the network without necessitating large scale reordering of the network in order to accommodate the particles. A consequence of the reduction in free-volume will however be that as the network goes through T_g, segmental motion will be inhibited by the presence of the nanoscale particles (though the effect is presumably too small in this case to have been observable by DSC). At low loadings of m-CB, the free volume for the network is reduced and there is a significant reinforcement effect with an increase in compressive strength. At higher temperatures large-scale multisegment co-operative motions will be influenced in a similar manner.

As the filler loading is increased there the mechanism of reinforcement may be expected to change or to be augmented by additional mechanisms. This would be expected at higher loadings simply because the network will be inevitably altered and perturbed by the increased levels of filler present. At this stage the reinforcement might be best described by invasive nanoscale reinforcement and the situation will be one whereby we see a combination of free-volume space filling *and* the development of a more conventional nanocomposite structure whereby the network is significantly altered to include the increased fraction of particles. Such a transition from noninvasive space filling to invasive space filling has been observed in an other nanocomposite system based on polyhedral oligomeric silsesquioxanes (POSS), though with a significant plasticization effect.[19] We did not observe this direct transition in our study, but at high filler loadings observed evidence of particle agglomeration. The size of the agglomerated partlicles was not measured, but we expect sizes >50 nm based on preliminary POSS Raman microscopy studies.[19] At these levels, the restriction in chain mobility observed is likely to be due in no small part to larger scale polymer−filler interface interac-

tions. At higher fill levels agglomeration of the m-CB begins to dominate and the modulus and residual dipolar couplings begin to decrease as a result. The propensity for these spherical fillers to be mobile and to migrate and agglomerate is documented by the TGA results and is supported by recent modeling results.[56,57]

References and Notes

(1) Petrovic, Z. S.; Javni, I.; Waddon, A. *Proc. ANTEC* **1998**, 2390.
(2) Heinrich, G; Klüppel, M. *Adv. Polym. Sci.* **2002**, *160*, 1.
(3) Nielsen, L. E.; Landel, R. F. *Mechanical Properties of Polymers and Composites*, 2nd edition; CRC Press: Boca Raton, FL, 1994.
(4) Joshi, M.; Bhupendra, S. B. *J. Macromol. Sci., Part C: Polym. Rev.* **2004**, *44*, 389.
(5) Ozmusul, M. S.; Picu, C. R.; Sternstein, S. S.; Kumar, S. K. *Macromolecules* **2005**, *38*, 4495.
(6) Flory, P. *Viscoelastic Properites of Polymers*, 3rd ed.; Wiley: New York, 1980.
(7) Erman, B.; Mark, J. E. *Structures and properties of rubber like network*; Oxford: New York, 1997.
(8) Kloczkowski, A.; Sharaf, M. A.; Mark, J. E. *Chem. Eng. Sci.* **1994**, *49*, 2889.
(9) Yuan, Q. W.; Kloczkowski, A.; Mark, J. E.; Sharaf, M. A. *J. Polym. Sci., Polym. Phys.* **1996**, *34*, 1647.
(10) Nakatani, A. I.; Chen, W.; Schmidt, R. G.; Gordon, G. V.; Han, C. C. *Polymer* **2001**, *42*, 3713.
(11) Vacatello, M. *Macromolecules* **2001**, *34*, 1946.
(12) Vacatello, V. *Macromolecules* **2002**, *35*, 8191.
(13) Ozmusul, M. S.; Picu, R. C. *Polymer* **2002**, *43*, 4657.
(14) Picu, R. C.; Ozmusul, M. S. *J. Chem. Phys.* **2003**, *118*, 11239.
(15) Sternstein, S. S.; Zhu, A.-J. *Macromolecules* **2002**, *35*, 7262.
(16) Blythe, A. R. *Electrical Properties of Polymers*; Cambridge University Press: Cambridge, 1979; pp 3959.
(17) Adachi, H.; Adachi, K.; Ishida, Y.; Kotaka, T. *J. Appl. Polym. Sci.: Polym. Phys. Ed.* **1979**, *17*, 851.
(18) Fragiadakis, D.; Pissis, P.; Bokobza, L. *Polymer* **2005**, *46*, 6001.
(19) Lewicki, J. P.; Patel, M.; Morrell, P.; Liggat, J. J.; Murphy, J.; Pethrick, R. A. *Sci. Technol. Adv. Mater.* **2007**, in press.
(20) Schmidt-Rohr, K.; Spiess, H. W. *Multidimensional solid-state NMR and polymers*; Academic Press: San Diego, 1994.
(21) Cohen-Addad, J. P. *Prog. Nucl. Magn. Reson. Spectrosc.* **1993**, *25*, 1.
(22) Saalwächter, K. *Prog. Nucl. Magn. Reson. Spectrosc.* **2007**, *51*, 1.
(23) Grinberg, F.; Garbarczyk, M.; Kuhn, W. *J. Chem. Phys.* **1999**, *111*, 11222.
(24) Schneider, M.; Gasper, L.; Demco, D. E.; Blumich, B. *J. Chem. Phys.* **1999**, *111*, 402.
(25) Sotta, P.; Deloche, B. *Macromolecules* **1990**, *23*, 1999.
(26) Fechete, R.; Demco, D. E.; Blumich, B. *J. Magn. Reson.* **2004**, *169*, 19.
(27) Dollase, T.; Graf, R.; Heuer, A.; Spiess, H. W. *Macromolecules* **2001**, *34*, 298.
(28) Fechete, R.; Demco, D. E.; Blumich, B. *J. Chem. Phys.* **2003**, *118*, 2411.
(29) Hafner, S.; Demco, D. E.; Kimmich, R. *Solid State NMR* **1996**, *6*, 275.
(30) Saalwächter, K.; Ziegler, P.; Spyckerelle, O.; Haidar, H.; Vidal, A.; Sommer, J.-U. *J. Chem. Phys.* **2003**, *119*, 3468.
(31) Saalwächter, K. *J. Chem. Phys.* **2004**, *120*, 454.
(32) Callaghan, P. T.; Samulski, E. T. *Macromolecules* **1997**, *30*, 113.
(33) Callaghan, P. T.; Samulski, E. T. *Macromolecules.* **2000**, *33*, 3795.
(34) Gjersing, E.; Chinn, S.; Maxwell, R. S.; Giuliani, J. R.; Herberg, J.; Eastwood, E.; Bowen, D.; Stephens, T. *Macromolecules* **2007**, *40*, 4953.
(35) Giuliani, J. R.; Gjersing, E.; Chinn, S. C.; Maxwell, R. S. *J. Phys. Chem. B* **2007**, *111*, 12977.
(36) Jagadeesh, B.; Demco, D. E.; Blumich, B. *Chem. Phys. Lett.* **2004**, *393*, 416.
(37) Wang, M.; Bertmer, M.; Demco, D. E.; Blumich, B.; Litvinov, V. M.; Barthel, H. *Macromolecules* **2003**, *36*, 4411.
(38) Chinn, S. C.; DeTeresa, S.; Sawvel, A.; Shields, A.; Balazs, B.; Maxwell, R. S. *Polym. Degrad. Stab.* **2006**, *91*, 555.

(39) Patel, M.; Swain A. C. *Boron-Containing Polymers*, Vol 8; Wiley-Interscience: London, **2007**.

(40) Brook, M. A. *Silicon in Organic, Organometallic, and Polymer Chemistry*; John Wiley & Sons: New York, 2000.

(41) Hayward, D.; Gawayne, M.; Mahboubian-Jones, B.; Pethrick, R. A. *J. Phys. E: Sci. Instrum.* **1984**, *17*, 683.

(42) Van Beek, L. K. H. *Prog. Dielectr.* **1967**, *7*, 69.

(43) Bell, W.; Daly, J.; North, A. M.; Pethrick, R. A.; Teik, P. B. *J. Chem. Soc., Faraday Trans. 2* **1979**, *75*, 1452.

(44) Oeser, R.; Ewen, B.; Richter, D.; Farago, B. *Phys. Rev. Lett.* **1988**, *60*, 1041.

(45) Sommer, J.-U. *Prog. Colloid Polym. Sci.* **1992**, *90*, 43.

(46) Grassley, G. *Macromolecules* **1980**, *13*, 372.

(47) Higgins, J. S.; Ma, K.; Hall, R. H. *J. Phys. C: Solid State Phys.* **1981**, *14*, 4995.

(48) Havriliak, S.; Negami, S. *Polymer* **1967**, *8*, 161.

(49) Macdonald, J. R. *Complex Nonlinear Least Squares. Immittance, Inversion and Simulation Fitting Programs for Windows and MS-DOS*; Solartron Group: Hampshire, U.K., 1999.

(50) Baum, J.; Pines, A. *J. Am. Chem. Soc.* **1986**, *108*, 7447.

(51) Grassie, N.; Macfarlane, I. G. *Eur. Polym. J.* **1978**, *14*, 875.

(52) Grassie, N.; Macfarlane, I. G.; Francey, K. F. *Eur. Polym. J.* **1979**, *15*, 415.

(53) Palsule, A. S.; Clarson, S. J.; Widenhouse, C. W. *J. Inorg. Organomet. Polym.* **2008**, *18*, 207.

(54) Patel, M.; Morrell, P. R.; Murphy, J. J. *Polym. Degrad. Stab.* **2005**, *87*, 201.

(55) Daly, J. H.; Guest, M. J.; Hayward, D.; Pethrick, R. A. *J. Mater. Sci. Lett.* **1992**, *11*, 1271.

(56) Lacevic, N.; Gee, R.; Saab, A.; Maxwell, R. S. *J. Chem. Phys.* **2008**, submitted for publication.

(57) Starr, F. W.; Douglas, J. F.; Glotzer, S. C. *J. Chem. Phys.* **2003**, *119*, 1777.

(58) Lewicki, J. P.; Liggat, J. J.; Hayward, D.; Pethrick, R. A. Patel, M. *Polymer Degradation and Stabilization*, ACS Symposium Series; American Chemical Society: Washington, DC, 2007; in press.

(59) Mark, J. E. *Adv. Polym. Sci.* **1984**, *65*, 136.